

Multi-modal Representation Learning Enables Accurate Protein Function Prediction in Low-Data Setting

Serbulent Ünsal^{*1,2}, Sinem Özdemir¹, Bünyamin Kasap³, M. Erşan Kalaycı¹, Kemal Turhan¹, Tunca Doğan^{†4,5}, and Aybar C. Acar^{‡2}

¹Department of Biostatistics and Medical Informatics, Faculty of Medicine, Graduate School of Health Sciences, Karadeniz Technical University, Trabzon, Türkiye

²Cancer Systems Biology Laboratory (KanSiL), Graduate School of Informatics, Middle East Technical University, Ankara, Türkiye

³Health Sciences University Trabzon Kanuni Training and Research Hospital, Medical Microbiology Laboratory, Trabzon, Türkiye

⁴Biological Data Science Lab, Dept. of Computer Engineering, Department of Computer Engineering, Hacettepe University, Ankara, Türkiye

⁵Dept. of Bioinformatics, Graduate School of Health Sciences, Hacettepe University, Ankara, Türkiye

Abstract

In this study, we propose HOPER (HOListic ProtEin Representation), a novel multimodal learning framework designed to enhance protein function prediction (PFP) in low-data settings. The challenge of predicting protein functions is compounded by the limited availability of labeled data. Traditional machine learning models already struggle in such cases, and while deep learning models excel with abundant data, they also face difficulties when data is scarce. HOPER addresses this issue by integrating three distinct modalities—protein sequences, biomedical text, and protein-protein interaction (PPI) networks—to create a comprehensive protein representation. The model utilizes autoencoders to generate holistic embeddings, which are then employed for PFP tasks using transfer learning. HOPER outperforms existing methods on a benchmark dataset across all Gene Ontology categories, i.e., molecular function, biological process, and cellular component. Additionally, we demonstrate its practical utility by identifying new immune-escape proteins in lung adenocarcinoma, offering insights into potential therapeutic targets. Our results highlight the effectiveness of multimodal representation learning for overcoming data limitations in biological research, potentially enabling more accurate and scalable protein function prediction. HOPER source code and datasets are available at <https://github.com/kansil/HOPER>

*serbulentu@gmail.com

†tuncadogan@gmail.com

‡acacar@metu.edu.tr

1 Introduction

Proteins are macromolecules that are the building blocks and essential machinery of life. However, knowledge about the functional properties of proteins is still limited. In particular, the UniProt knowledgebase, the largest information hub for proteins, has approximately 250 million protein records; however, only 0.3% of them are manually reviewed. Manual annotation of protein function requires wet lab experiments and curation of results by human experts. This is a slow and high-cost process. Especially in the last decade, rigorous efforts have been made to annotate proteins with automated systems (a.k.a protein function prediction – PFP) [1, 2, 3]. Machine learning (ML) based protein function prediction has two major issues. First, there is a need for data preprocessing, since conventional ML methods rely on manually extracted features (e.g., physicochemical properties of proteins). Second, the predictive accuracy of these methods is still not sufficient, as indicated by the CAFA (Critical Assessment of Functional Annotation) challenge, which is a well-known and periodic PFP competition [4] based on Gene Ontology (GO) annotations [5, 6] for molecular function (MF), biological process (BP) and cellular component (CC) categories. Consequently, PFP is still an open problem.

Deep learning techniques, on the other hand, not only display high performance in biological data modelling but also eliminate the need for manual feature extraction [7, 8, 9]. However, one important problem of deep learning models is requiring extensive labelled training datasets to achieve high accuracy [10, 11]. The lack of large-scale data hampers the effectiveness of deep learning in PFP, prompting researchers to explore alternative strategies to address this limitation. Even though there are a few PFP studies that consider the low-data problem, e.g., DEEPred [12], DeepGOZero [13] and ProTranslator [14], none of them demonstrated adequate generalisation in practical scenarios. Hence, new methods are needed for low-data PFP that use integrative approaches. Additionally, a variety of machine learning algorithms have been proposed to solve the data problem, such as few-shot learning [15], generating synthetic data [16], one-shot learning using Siamese network [17], data-efficient reinforcement learning [18]. Applications of these approaches include predicting the effects of mutations [19], acetylation site prediction [20], predicting kinase-phosphosite associations [21], protein localisation prediction [22], and protein design [23]. Nevertheless, these solutions are mostly problem-specific; hence, for each task, new models should be trained and fine-tuned from scratch. This process is costly in terms of time and funds.

An alternative solution for the problem of large data requirements is representation learning. In this approach, a model is pre-trained using a large dataset of unlabeled samples. Thus, a generalised high-dimensional representation of the input data is learned. This pre-trained model can be used in subsequent prediction tasks [24] by either fine-tuning the original model or training a new supervised model that utilises the representations/embeddings produced by the pre-trained model as input. These representations can capture various critical biochemical and functional features of proteins. As an example, Vig et. al. [25] investigated the transformer architecture [26] in this context and found out that

attention layers can capture valuable information on structure, contact points, binding sites and evolutionary information. These findings were supported by others, who added function prediction to this list through deep mutational scanning data [27] and fitness landscapes [28].

Most protein representation learning (PRL) models solely use protein sequence data as input, which is information-rich; however, part of this knowledge is implicit, which is difficult to extract. Other data types, such as the natural language-based text from the biomedical literature and molecular relationships (e.g., protein-protein interactions), can explicitly contain protein-related information. Therefore, leveraging multiple data types has the potential to improve protein learning.

Multimodal representation learning, defined as the extraction of knowledge from a combination of data modalities, is a promising approach utilised in various fields of data science [29]. Techniques such as early and late fusion [30], multiplicative interactions [31], multimodal gated units [32], temporal attention [33] (a.k.a multimodal transformers), architecture search [34] have been employed to yield integrative learning with multiple modalities in the literature. Additionally, alternative training procedures, i.e., gradient blending and regularisation [35] by maximising functional entropies [36], have been used. An evaluation of these approaches can be found in the MultiBench study [37].

Multimodal learning has also been exploited in the framework of biological sequence analysis, such as the prediction of (i) long noncoding RNA-Protein interactions with capsule networks [38], (ii) long noncoding RNA-miRNA interactions [39], (iii) protein ubiquitination sites [40], (iv) protein-protein interactions [41, 42], (v) moonlighting proteins [43], and (vi) small molecules of novel scaffolds sharing similar target biological activities [44].

In this study, we proposed a holistic protein representation learning model, HOPER, using multimodal learning to perform high-performance PFP even with low training data. The outline of our study is given in Figure 1. For this, we first created representation vectors using (i) amino acid sequences, (ii) protein-based text from the literature, and (iii) protein-protein interaction data types. We then yielded integrative (multimodal) learning over those three modalities using autoencoders. The amino acid sequences of proteins have already been the main type of input data for most of the protein representation learning methods in the literature. The rationale behind incorporating protein-protein interactions into our model is the assumption that interacting proteins are likely to act in the same biological process and cellular component. Apart from that, the reason for utilising textual data from the scientific literature is that it contains rich knowledge directly refined from experimental (wet-lab) results. Such data may include a comprehensive semantic context for the given protein.

Additionally, we showed that once the sequence is enriched with text and PPI data, this associative knowledge can be used to develop high-performing sequence-based low-data PFP models via transfer learning when text and PPI data are unavailable. This model was developed mainly to learn the relationship between sequence and other modalities. Our HOPER models were tested on

a PFP benchmark (using the GO categories of MF, BP, and CC), which was explicitly designed to evaluate protein representation learning methods under different training sample sizes (low, middle, high) and function specificity levels (specific, normal, shallow). Finally, as a use case, we employed HOPER to identify new immune-escape proteins in the lung adenocarcinoma disease.

2 Results

Our multimodal protein representation model, HOPER (Holistic Protein Representation), uses sequence, text, and PPI as data modalities. Here, we investigated the performance of HOPER and its constituents on the problem of Gene Ontology-based protein function prediction (PFP). We developed and tested a variety of models to combine these modalities, especially using multimodal learning approaches.

We utilised our previously constructed benchmarking framework, PROBE (Protein RepresentatiOn BEenchmark), for PFP performance evaluation and comparison [45]. PROBE was constructed to identify how protein representation models performed on PFP problems under different function specificities and different training dataset sizes. We carefully curated nine different protein function datasets considering sample counts (i.e., low, middle, and high), and GO term specificities (i.e., specific, normal, shallow). We selected groups of GO terms (mostly composed of 5 terms for each group) based on combinations of these two parameters. The benchmark framework covers the molecular function (MF), biological process (BP), and cellular component (CC) aspects of GO. For instance, the benchmark dataset referred to as “MF_Low_Shallow” includes 5 MF GO terms that are closer to the root of the GO MF tree (i.e., “shallow” in terms of term specificity), each of which has 5 to 30 protein annotations (i.e., “low” in terms of the number of samples). Details about the other datasets and the included GO terms can be found in the Methods section.

Below, we first explain the results of the PFP analyses done independently on three different types of data modalities. Then, we elaborate on the multi-modal learning approaches we utilised to yield holistic learning over the sequence, PPI, and text modalities and their subsequent PFP benchmark performance outcome.

2.1 Evaluation of sequence-based representation models

We evaluated 23 protein representations using the PROBE benchmark [45]. We employed a linear classifier to decouple the classification’s final performance from the representation model. We utilized a linear boundary classifier to ensure that the test results accurately reflect the models’ ability to learn meaningful high-dimensional representations of the protein space. The ideal representation should ensure that the proteins’ functional properties are linearly separable.

Figure 2 and Supplementary Table S1a display the GO prediction performance

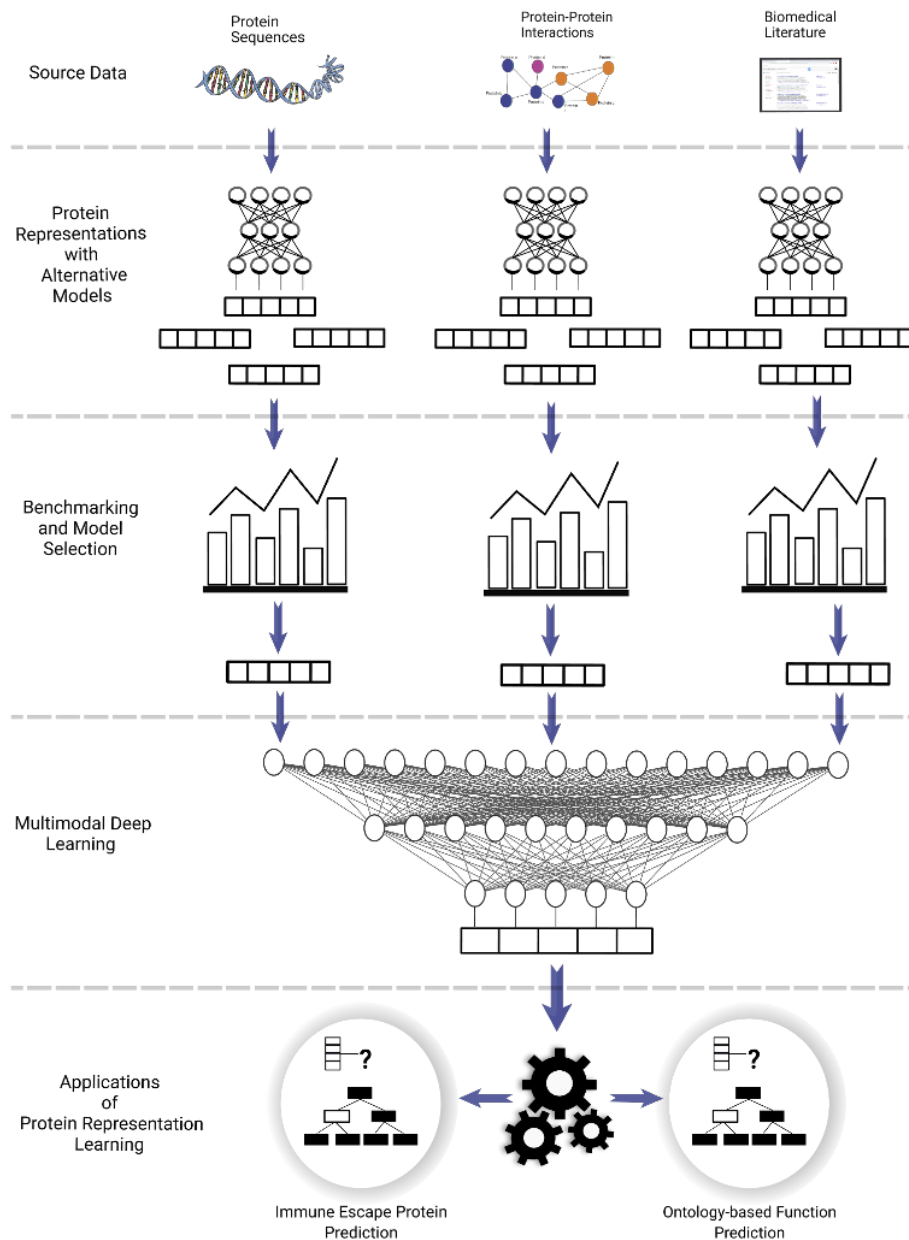


Figure 1: The overview of the study. We first generated protein representations (embeddings) independently using three different modalities (i.e., protein sequence, protein-protein interaction, and text). Then, we benchmarked them to find the best-performing representation model for each modality in the context of protein function prediction in low training data setting. After that, we constructed multimodal learning models that take representations of independent modalities as input and produce a holistic embedding by leveraging their relationships. Finally, as a use-case study, we predicted new tumor immune-escape proteins in the lung adenocarcinoma disease using our model and discussed the results.

results of 23 protein representations. In the benchmark, learned representation models generally outperformed classical methods, especially in predicting Molecular Function (MF) GO terms. Performance was lower for Cellular Component (CC) and Biological Process (BP) predictions, likely due to the reliance on sequence data, which isn't a strong indicator for these tasks. Prediction accuracy declined with fewer annotated proteins, particularly for CC terms, but there was no clear difference based on term specificity. However, challenges remain in predicting specific GO terms due to limited annotation. Our evaluation of various PFP methods for predicting Gene Ontology (GO) terms revealed that some of the protein language models (e.g., ProtT5-XL, ProtALBERT, SeqVec, ProtBERT, etc.) outperformed classical methods (e.g., BLAST, KSEP, etc.) significantly. We observed that the success rate in predicting GO terms decreased with fewer annotated proteins (i.e., smaller training datasets), especially for specific/informative terms. Despite this, we found that some of the top-performing methods demonstrated consistent performance across virtually all GO groups, with ProtT5-XL [46] emerging as the best performer in all three categories (CC, BP, and MF), followed closely by ProtALBERT, SeqVec, ProtBERT-BFD, and HMMER.

2.2 Evaluation of protein-protein interaction-based representation models

For this analysis, the protein-protein interaction (PPI) data is encoded as a graph. We selected two widely used graph representation methods with reference code implementations, High-Order Proximity Preserved Embedding HOPE [47] and Node2Vec [48]. We applied these methods to the PPI graphs to calculate node (i.e., protein) representation vectors. We explored various hyperparameters for these methods and visualized the best performing 10 parameter combinations for each. Selected hyperparameters for the HOPE method are "d" and "beta". Likewise, "p", "q" and "d" are tuned for Node2Vec. We explain these hyperparameters in the Methods section.

The HOPE method has two aims: preserving high-order proximity and capturing asymmetric transitivity. On the other hand, Node2Vec uses a random walk and word2vec [49] to compute node embeddings in graphs. We used the IntAct database (accessed on September 6, 2020) to acquire PPI data and used only the interactions between human proteins. The final network includes 16,435 nodes (proteins) and 241,833 edges (protein-protein interactions).

Figure 3 and Supplementary Table S1b show that Node2Vec was more accurate than HOPE on the PFP problem. A possible reason is a mismatch between the objectives of the HOPE model and the particulars of our use-case: The first objective of the HOPE is high-order proximity. However, in PPI networks, low-order proximities are more indicative of functional relationships. Similarly, HOPE's second objective, capturing the asymmetric transitivity, might not apply to our data since our graph is undirected.

Another important observation is the relation between hyper-parameters and

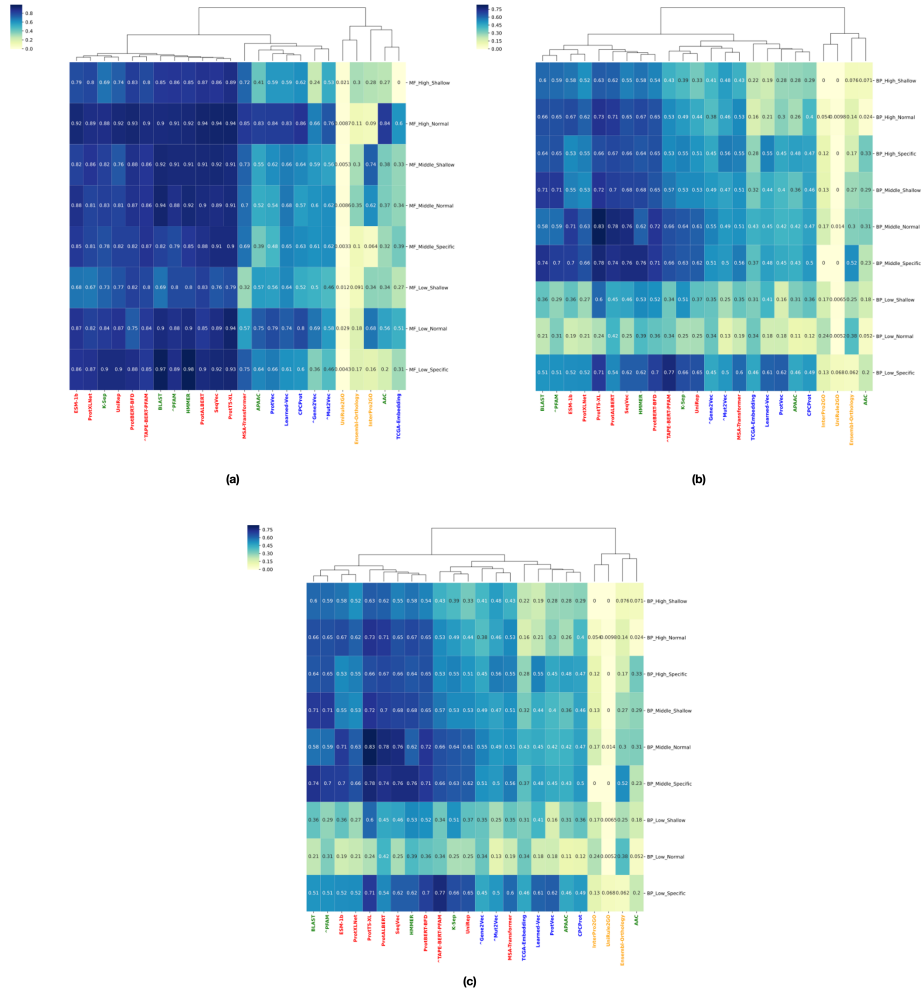


Figure 2: Ontology-based protein function prediction benchmark results. Heat maps indicating the clustered performance results (weighted F1-scores) of protein representation methods in ontology-based PFP benchmark in terms of GO categories of (a) molecular function, (b) biological process and (c) cellular component. The colours indicate groups of models (yellow, rule-based annotation methods; green, classical representations; blue, small-scale learned representations; red, large-scale learned representations).

model performance. As shown in Figure 3 and Supplementary Table S1b, model performance is sensitive to hyperparameters.

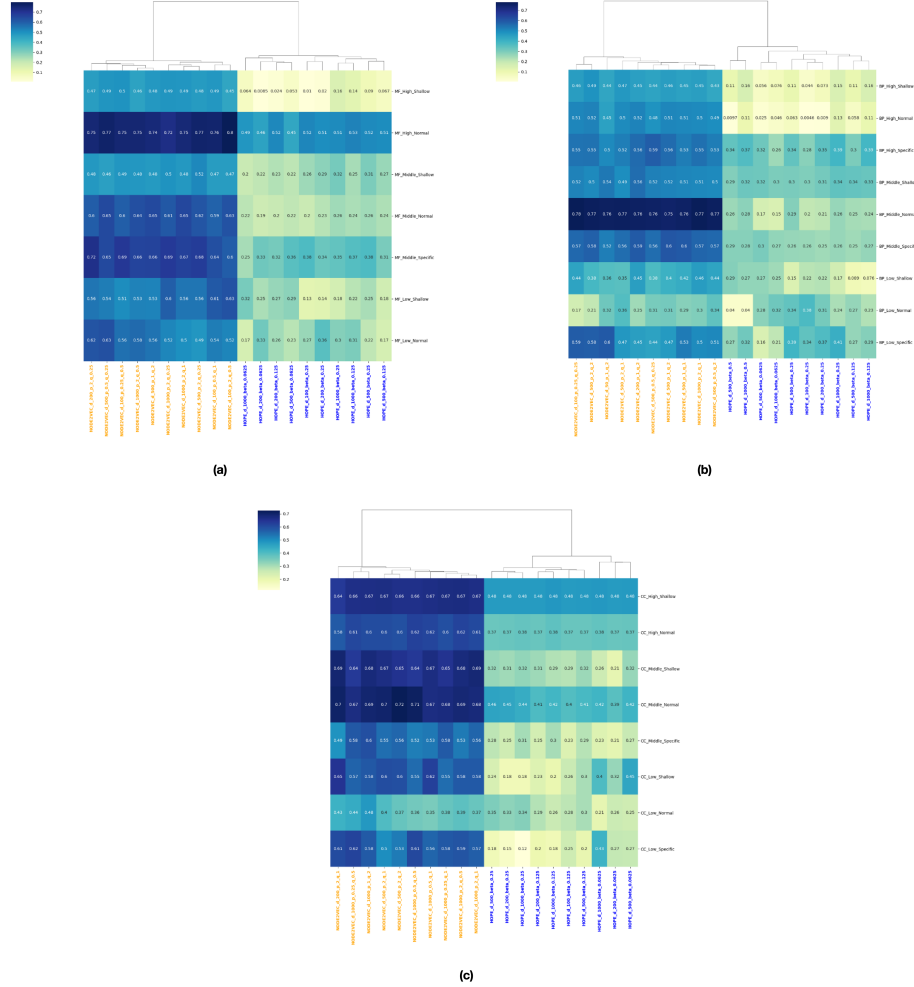


Figure 3: Protein function prediction performances of PPI representations based on mean F1-weighted scores. Multiple models that utilize Node2Vec and HOPE algorithms are shown with different hyperparameter selections (p and q for Node2Vec and beta for HOPE). Tests were conducted on the low data setting (i.e., MF, BP, and CC GO terms with low number of annotated proteins) for; **a** MF; **b** BP; and **c** CC terms.

2.3 Evaluation of text-based protein representation models

Text data, obtained either from curation or directly from the literature, can be considered one of the most refined data sources to acquire knowledge on protein functions. However, this information is highly distributed and heterogeneous. We aimed to incorporate this knowledge as a protein representation. To accomplish

this, we used two data sources; curated UniProt text from flat files (for 20,365 human protein records in total), and scientific literature (in the form of article abstracts) for selected human proteins using PubMed records of the articles cited in the curated text of the protein of interest in UniProtKB (17,639 protein records in total). We obtained text data from the “Comments section” for each human protein entry.

We evaluated alternative methods to calculate textual representations of the proteins in our dataset. First, we apply the term frequency–inverse document frequency TF-IDF [50] to the text data which is explained in the methods section. The size of the original TF-IDF vectors was determined according to the number of unique terms (mostly words) in the corpus. However, the resulting vectors were large (54428 dims for UniProtKB retrieved text and 178451 dims for UniProtKB&PubMed retrieved text) and processing them directly would have been both computationally intractable and might have caused problems due to the curse of dimensionality. To mitigate this problem, we applied principal components analysis (PCA) and constructed vectors composed of 256, 512 and 1024 principal components as “reduced TF-IDF vectors”. We called this method TF-IDF_PCA.

Afterwards, we used pre-trained text representation models to generate text-based protein representations. We first evaluated the BioWordVec [51] model which uses the classical word2vec algorithm and is pre-trained on the PubMed text corpus and MIMIC III data containing 2,324,849 distinct words in total. The number of dimensions in BioWordVec vectors is 200. We also utilized BioSentVec [52]. BioSentVec uses the sent2vec [53] model to compute 700-dimensional sentence embeddings and is trained on the same dataset as BioWordVec. Similarly, we utilized the BioBERT [54] model. The BioBERT model is a BERT [55] based model which is trained on biomedical and clinical corpus, more details can be found in the methods section. The BioBERT, BioWordVec, and BioSentVec produce representation vectors per word. We max-pooled or averaged these vectors for all words in the text data per protein.

We observed that TF-IDF_PCA produced the best performance on the PFP problem in the text-based models. The best performance with TF-IDF_PCA is achieved when UniProt and PubMed data are jointly used as the input. Even though TF-IDF_PCA is the most simplistic model and showed the top performance, the BioBERT, the most sophisticated and extensive sized model compared to other models we evaluated (according to number parameters), was the worst performed overall (Figure 4 & Supplementary Table S1c). In the natural language processing (NLP) domain, these approaches were successful, especially on data composed of short sentences [56]. However, models specialized in processing longer sequences are required here such as Longformer [57] and Reformer [58]. Unfortunately, none of the available long-sequence models are pre-trained in biomedical texts. On sub-category-based performance, all models underperformed in the “low-data” category. For other categories, no clear pattern was observed.

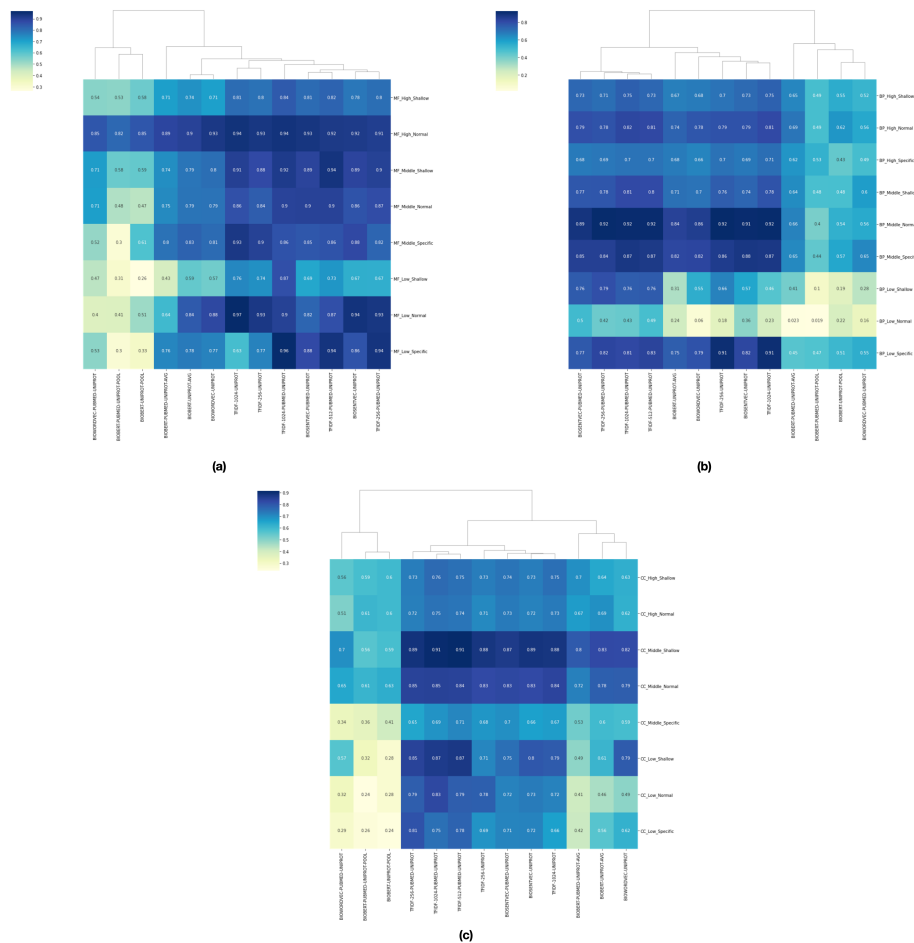


Figure 4: Protein function prediction performances of text-based representations based on mean F1-weighted scores. Multiple models that utilize TF-IDF-PCA, BioSentVec, and BioBERT algorithms are shown with different hyperparameter and data source selections. Tests were conducted on the low data setting (i.e., MF, BP, and CC GO terms with low number of annotated proteins) for; **a** MF; **b** BP; and **c** CC terms.

2.4 Generating a holistic protein representation using autoencoders

Currently, representations that aim to integrate multiple types of protein features (i.e multimodal models) are limited especially for PFP [59, 60, 43]. Moreover, according to the best of our knowledge, none of these models specialized in producing accurate predictions in a low-data setting. Another problem in the application of multimodal approaches is the scarcity of data, such as experimentally verified protein-protein interactions and curated biomedical texts. For example, in our study, we analyzed the human proteome, which is one of the most extensively studied protein collections in the literature. Here, a total of 20,421 proteins were found to possess sequence data, whereas 16,435 proteins exhibited PPI. Additionally, 17,639 proteins were annotated with textual information. Notably, 14,941 proteins were found to possess all three data types, thereby providing a multi-dimensional perspective of these proteins. Here, we aimed to circumvent these problems and develop multimodal models that can learn relationships between different types of protein data (i.e., text, PPI, and sequence) and generate holistic protein representations.

The first approach we considered for leveraging multiple modalities is a concatenation of representations generated by text, PPI, and sequence. We have created all subsets of these representations. The second approach we applied is training a simple autoencoder (Simple-AE) which takes a concentrated representation consisting of text, PPI, and sequence and aims to reconstruct the input representation (Figure 5a). The third approach we used was a multimodal autoencoder (MultimodalAE), which takes input from each modality separately, encodes it using its shared middle layer, and tries to reconstruct each representation separately (Figure 5b). The fourth approach we applied was a transfer learning-based multimodal sequence autoencoder. We named this model TransferAE (Figure 5c). At the end of their training procedures, we used the bottleneck layer of these autoencoders as our protein representations and utilized them in our PFP models. We compared numerous representations with varying bottleneck sizes to optimize PFP performance. We trained a simple linear support vector machine (SVM) model as the protein function predictor.

Figure 6 and Supplementary Table S2 show that the simple autoencoder model (Simple_AE_512) performed best in the MF category. For the BP and CC categories, TF-IDF_PCA produced the best performance. The difference between TF-IDF_PCA and simple autoencoder models was not significant. These results indicate that none of the multimodal models were able to attain a synergistic effect to outperform text. One other reason might be a suspected data leak from text to Gene Ontology terms, which we will elaborate on in the discussion section.

When comparing the best sequence-based model (ProtT5-XL) with TransferAE_768, the latter demonstrates significantly improved performance in the low category, with weighted F1-scores of 0.92 vs. 0.85 for MF, 0.68 vs. 0.55 for BP, and 0.68 vs. 0.61 for CC. Detailed results are provided in Supplementary Table S2. Here, our primary goals were, (i) developing a multimodal model

for functions that have a low-number of samples (i.e., proteins annotated to the function of interest), and (ii) have the capability to assign functions to understudied proteins (e.g., proteins for which only sequence data is available). Therefore, these goals were satisfied with the TransferAE model.

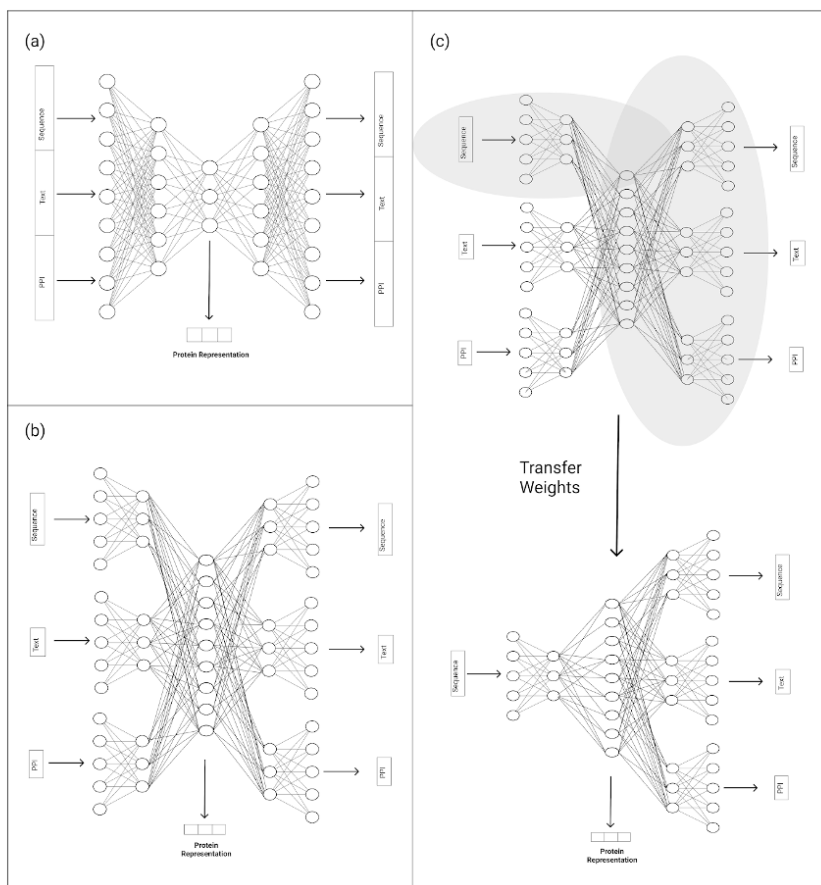


Figure 5: Construction of multimodal representations using autoencoder models; **a** simple autoencoder (SimpleAE), **b** multimodal autoencoder (MultiModelAE), and **c** transfer learning-based sequence-input multimodal autoencoder (TransferAE).

Finally, we visualized the best-performing representations (i.e., SimpleAE_512 for MF and ProtT5-XL + Node2Vec + TF-IDF_PCA for BP and CC) on the 2-D plane for each protein function dataset. We employed the t-SNE algorithm [61] for dimensionality reduction. The scikit-learn (v1.2.1) manifold TSNE module is used with default parameters. Resulting density plots showed how well each term could be separated by the representation at hand (Figure S1).

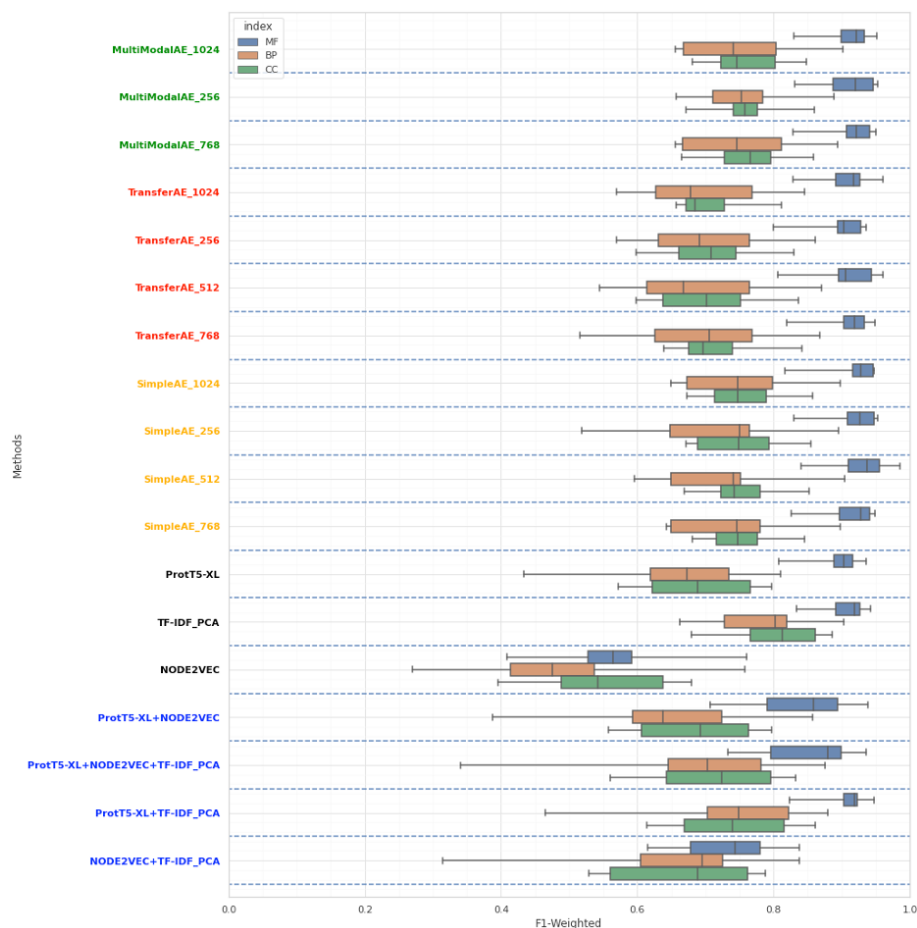


Figure 6: Overall performance evaluation of multimodal protein representations in protein function prediction, based on mean F1-weighted scores. The study showcases various models; black: the best performing single modality, blue: fused (FusedRep), yellow: simple autoencoder (SimpleAE), green: multimodal autoencoder (MultiModalAE), and red: transfer learning-based autoencoder (TransferAE) representation models with varying embedding dimension sizes. The tests were conducted on the Gene Ontology (GO) categories of molecular function – MF (blue bars), biological process – BP (orange bars), and cellular component – CC (green bars), considering all dataset size and term specificity-based groups.

2.5 Case Study: Immune Escape Protein Prediction

As a case study, we aimed to predict new immune escape proteins in lung adenocarcinomas, which is the cancer type with the highest mortality rate [62]. Immune escape can be defined as a tumor’s ability to evade immune elimination [63]. Although this mechanism has critical importance in cancer research, the current knowledge of it is not sufficient to develop a broad spectrum of therapeutics. Related to this, the current number of proteins that are known to take part in immune escape is limited (28 proteins considering all types of cancer). Therefore, there is a current requirement to discover other proteins that take part in immune escape. This problem can be considered a good example of the critical requirement to develop a prediction model with a low amount of training data.

To accomplish this task, we conducted the following steps; (i) We obtained differentially expressed genes for the lung adenocarcinoma using TCGA-LUAD dataset RNA-Seq data [64], which constituted our positive dataset; (ii) created the positive and negative samples datasets; (iii) constructed our main immune escape prediction model by taking the multimodal representations from our best performing AE-based representation model for low-data (which was found in the previous analysis shown in Supplementary Table S2) and trained FC-NN using these vectors as input and (v) analyzed results via literature search and existing functional annotations in source databases.

The detailed process is explained below for each step;

(i) We acquired TCGA-LUAD RNA-Seq data as stated above and calculated fold changes using read counts. We used the General Linear Model (GLM) and fit read counts to a negative binomial distribution before testing them to find significance scores for the calculated fold changes. We applied the glmLRT function from the EdgeR package for these steps. Hence, we obtained log fold-change (logFC) scores and respective false discovery rates (FDRs) at the end of this process.

In the end, we found 1434 differentially expressed genes, of which 329 were low, and 1105 were highly-expressed in lung adenocarcinoma tumors compared to the matched normal lung tissue (Hoper Differentially Expressed LUAD Genes) (Supplementary File 1).

(ii) We created our own positive and negative training datasets. We curated 24 proteins from the literature that is known to take part in the immune escape process (Supplementary Table S11). Our initial negatives candidate set consists of human proteins that have GO BP annotations. Using Uniref50 clusters we selected representative proteins from our candidate set. So, we ensure that none of the candidates have a sequence similarity of more than 50% against each other. Afterwards, we calculate semantic similarity of each protein to the known immune-escape proteins using Lin similarity [65] and GO Biological Process (BP) ontology. Then we create a set from these proteins which have less than

50% semantic similarity with the positive set (known immune-escape proteins), on average. Finally, we chose 150 proteins from this set randomly to create a dissimilar but diverse set of negative samples (Supplementary Table S12)¹.

(iii) Using our best autoencoder-based representation (i.e., MultiModalAE-256), we trained immune-escape predictors models within a hyperparameter search. We utilized fully connected feed-forward neural networks (FC-NN), to predict new immune-escape proteins. We accrued macro-averaged precision 0.80, macro-averaged recall 0.72 (Supplementary Table S7). Using this model, we predicted possible immune-escape proteins among the differentially expressed gene set. In the end, we positively predicted 121 proteins from 1434 differentially expressed genes/proteins. These proteins were evaluated with a literature search, and 20 potential LUAD immune-escape therapy targets were identified (Supplementary Table S4). Below, we discussed two of these proteins in the framework of a literature survey.

One of the positively predicted proteins, matrix metalloproteinase 9 (MMP9) has recently been suggested as a potential therapeutic target for cancer immunotherapy due to its role in tumor escape from anti-angiogenic therapies. MMP9 plays an important role in the angiogenesis, invasion, and immune escape of tumors and has been studied in relation to the production of type IV and type V collagens in the extracellular matrix. This increases the vascularization of tumors, resulting in increased tumor growth. Additionally, MMP9 increases the production of Treg cells, which further aids in tumor invasion. MMP9 stimulates the release of cytokines, which activate the production of Treg cells. The increased Tregs then suppress the normal immune response and allow the tumor to escape the body’s defenses [66]. Further investigation of MMP9 revealed that it cleaves the osteopontin isoform and increases the number of Myeloid-derived suppressor cells (MDSC) in the tumor tissue, suppressing the immune response and allowing the tumor to escape the effects of immunotherapies. MMP9 first cleaves the osteopontin isoform, which in turn stimulates the release of pro-inflammatory cytokines. These cytokines then activate MDSC proliferation, leading to an increase in their numbers. Hence, MMP9 is a key player in the angiogenesis, invasion, and immune escape of tumors and could be a potential drug target for cancer immunotherapy [67]. Here, a critical observation is our model’s prediction of MMP3 also as an immune-escape protein. Our further investigation showed that MMP3 is an activator of pro-MMP9 [68]. Hence, our model has the capacity to predict multiple actors of the immune-escape pathways.

Another protein that is predicted by our FC-NN model to play a role in the immune escape process, tumor necrosis factor ligand superfamily member 11 (TNFSF11 or RANKL), is a cytokine belonging to the TNF alpha cytokine family that binds to the TNFRSF11A/RANK receptor. RANKL is secreted directly by tumor tissue to create an immunosuppressive microenvironment in tumors and binds to RANK receptors on the surface of dendritic cells. This binding leads to the activation of a signaling pathway that ultimately results in the production of TGF β by the dendritic cells. The signaling pathway activated by RANKL

¹See PROBE study “Ontology-based Protein Function Prediction Benchmark” subsection under the Methods section for details.

involves several intermediates, including TRAF6, NF κ B, and MAP kinases. These intermediates ultimately activate the Smad family of transcription factors, which are involved in the regulation of TGF β expression [69]. TGF β binds to receptors on the surface of T cells, which activates a signaling pathway that leads to the expression of Foxp3, a transcription factor that is necessary for the development and function of TREG cells [70]. Hence, once TGF β is produced, it acts on T cells to promote the differentiation of TREG cells which suppress T Cells and causes immune-escape. Overall, the pathway from high levels of RANKL to the formation of TREG cells causes immune suppression and tumor immune-escape as well.

Apart from positively predicted proteins, successfully predicting negative samples is a critical task. The immune system is wide and complex, involving numerous proteins (1,500 [71]), thus, it can be challenging to prove that a specific protein is not related to immune system function. We explored negative examples to elucidate the limited relationships between the proteins of interest and the immune system. These are the proteins that exist in our input list (i.e., the ones that were differentially expressed in the lung adenocarcinoma), but are predicted not to play a role in immune escape by the FC-NN model. One such protein is AKR1C2, a member of the aldo/keto reductase superfamily that catalyzes the conversion of aldehydes and ketones to alcohols. While AKR1C2 is indirectly associated with myeloid-derived suppressor cells (MDSC) via PGE2, it is not directly involved in immune system function [72]. Collagens, including COL1A1, COL3A1, COL5A1, COL5A2, and COL11A1, are structural proteins that provide strength and stability to tissues. Although collagens are present throughout the body, they do not primarily participate in immune system function except for infiltration [73]. A second example, ALB (albumin) is synthesized in the liver and primarily functions as a transporter for various substances such as drugs and hormones. While the liver has immune-related functions, ALB’s primary role is not directly related to the immune system [74]. A third example, CPS1 (carbamoyl phosphate synthetase 1) is an enzyme that facilitates the removal of excess nitrogen from the body via the urea cycle. Even though this process is important for health and homeostasis as a whole, CPS1 does not directly affect the immune system, even though some studies have looked at the relationship between nitrogen metabolism and the immune system [75]. Finally, CALCA (Calcitonin gene-related peptide 1) is a peptide hormone that regulates calcium and phosphate metabolism in bones. While calcium and phosphate are crucial for immune function [76, 77], CALCA itself does not directly participate in the immune system.

3 Discussion

In this study, we aimed to address the challenge of predicting protein functions with a limited amount of training data by developing multimodal protein representations. To validate the efficacy of these representations, we created a benchmarking tool capable of evaluating their performance in the context of low-data protein function prediction (PFP). Through the examination of various

representation modalities and methods, we demonstrated the usefulness of our multimodal protein representations. As a case study, we applied these representations to the task of predicting immune-escape proteins in lung adenocarcinoma, showcasing their ability to assist in answering research questions despite the constraints of limited data availability.

Our sequence-based multimodal representation demonstrates superior performance compared to alternative approaches for low-data protein function prediction.

Our overall benchmarking results revealed that a simple text-based representation (TF-IDF_PCA) achieved the best performance for predicting gene ontology (GO) biological process (BP) and cellular component (CC) terms. This method was also nearly as successful as the best method for predicting molecular function (MF) terms. Unexpectedly, text-based representations outperformed multimodal representations, which may be the result of an indirect data leak. The wet-lab results extracted from scientific literature are used both to generate the curator-written text data offered by UniProt and to assign GO annotations to proteins, which may have caused an unfair advantage to text-based representations. The only exception to this was the MF category, where the sequence-based representations performed better, probably due to the direct relationship between the protein sequence/structure and the molecular function it performs (e.g., presence of a kinase domain indicating the protein’s amino acid phosphorylation function – GO:0006468).

A comparison among text-based representation models revealed that, the most basic approach, term frequency-inverse document frequency (TF-IDF), demonstrated higher performance than more complex methods such as BioBERT in all subcategories of low-data PFP including MF, BP, and CC. One potential explanation for this result is the pooling process used by large language models like BioBERT [54]. These models generate a representation vector of size N for each word in a text, resulting in a matrix with dimensions $L \times N$ for a text with L words. This matrix must then be pooled into a fixed-size vector of N dimensions. One common method for pooling is to take the average of all vectors in the matrix, which can capture the overall meaning of the text, but may also result in information loss for long texts. Alternative pooling methods such as max pooling, which selects the maximum values for each dimension in the matrix, may also result in information loss in a similar manner. There are examples which TF-IDF or inverse document frequency (IDF) based approaches produce equal or better results than BERT [55] based solutions. For example, in a recent study researchers evaluated TF_IDF and BERT for long texts and multi-label document classification and observed that performance of the TF-IDF is better than the BERT model [78]. In another study the authors showed that for long legal text classification performance of TF-IDF and BERT is comparable and their approach combines inverse document frequency (IDF) and PCA performed better than the BERT model [79]. Finally, in another legal text classification study, a combined approach of TF-IDF and logistic regression showed better performance on multiple NLP tasks than the DistilBERT [80] model which is a BERT derived but more enhanced model [81].

In this study, our primary objective was to develop a novel protein function prediction (PFP) representation that is effective when the positive class in the training set is limited. This scenario, referred to as low-data PFP, presents a significant challenge for PFP methods. As mentioned above, in our analysis, the best method in terms of the mean results on all categories (i.e., not only considering the low data setting) was TF-IDF_PCA. When evaluating low-data PFP results, we observed an improvement in performance by SimpleAE and MultiModalAE over the leading baseline method, TF-IDF_PCA, for both GO MF and BP categories. These findings suggest that multimodal methods hold significant promise for improving PFP accuracy in low-data scenarios.

Although text-based models are generally effective in PFP, a major limitation of text data is its scarcity, particularly for under-studied proteins. To address this issue, we developed TransferAE, which can learn relationships between protein sequences and data generated by other modalities (e.g., protein-protein interaction and text from literature). When the results were analyzed, we found that TransferAE performed better than the best sequence-based (single modal) model ProtT5-XL [82], demonstrating the efficacy of our approach. Our results show that knowledge from multimodal models can be effectively transferred to sequence-only models, improving protein function prediction in low-data scenarios. This suggests that cross-modal pattern learning enhances performance, making multimodal approaches valuable for studying novel proteins where additional modality-based data is limited.

Our case study indicates multimodal learning might have applications in research and the clinic.

In our case study, the objective was to develop a predictive model for identifying immune-escape proteins in lung adenocarcinoma using the proposed multimodal machine learning approach. We have used our best multimodal representation (MultiModalAE-256) for low-data GO BP PFP, and trained classification models that take this representation as input, using fully connected neural networks (FC-NNs). Our model was initially provided with a set of 1,434 potential proteins, from which it identified 121 immune-escape candidates. Of these, 20 were subsequently validated through literature analysis, underscoring the success and efficiency of our approach, which significantly reduces the time required for manual selection. It is worth noting that the time required for the selection of the 121 immune-escape protein candidates would be significantly longer if conducted manually. Given the importance of time in cancer research together with monetary costs of wet-lab experiments and clinical trials, our models have the potential to expedite the identification of potential therapeutic targets. By automatizing the process of candidate gene/protein selection, accurate computational predictions reduces the burden on human experts.

We validated a few positive and negative predictions of this model from the literature, which indicated that the model’s results have biological relevance. Nevertheless, it was not possible for us to perform a full literature-based validation on all of the predictions (similar to the one done on the 121 positive predictions of the baseline model), since manual inspection is both time- and labor-intensive, especially considering the estimated 1500 proteins that are involved in the human

immune system [71]. However, it is imperative to recognize that this lack of validation does not necessarily signify that our positive predictions are false positives, as they could be immune-escape proteins that are yet to be discovered or documented. This point is especially important considering the fact that precision scores of all models, including SVM, were measured extremely low, due to the high number of hits that were considered as false positives, which may turn out to be true positives after a thorough literature search. In a similar fashion, given the complex nature of the human immune system and their neighborhood in the context of PPIs, our model’s negative predictions may still have relevance to the immune system and serve as immune-escape-related proteins under specific conditions. Despite these limitations, our primary objective remains to illuminate the unknown immune-escape protein space. Through the utilization of innovative machine learning approaches, our models are well-positioned to identify novel immune-escape proteins that may have been missed by traditional experimental methods.

Overall, our findings contribute to the growing body of literature on immune-escape proteins and provide new insights into potential targets for immunotherapy in lung adenocarcinoma.

4 Conclusion and Future Work

This study mainly investigates the potential of multimodal representation learning for low-data protein function prediction. Multimodal representation learning has become a major research direction in machine learning, attracting significant attention from researchers [71]. While previous works have mainly focused on designing fusion strategies to explore cross-modal interactions, these methods are limited in their ability to explicitly model complex cross-modal interactions [83]. In recent years, various modern fusion strategies have been developed to overcome this limitation, including tensor fusion multi-view RNN networks [84], modality-translation approaches [85], cross-modal attention mechanisms [86], graph-based fusion algorithms [87], and explainable fusion approaches [86, 88]. Meanwhile, multi-task multimodal learning frameworks have been proposed to capture the inherent correlation between different multimodal tasks and to help the model better understand the multimodal contents [83].

Furthermore, while autoencoders have been applied for representation learning in various domains, there are more complex methods such as variational autoencoders (VAEs) and generative adversarial networks (GANs) that have shown great potential for generating high-quality representations. These advanced models can offer improved performance for multimodal representation learning tasks.

While sequence-based models have shown promise, there is still much potential for improving single modality representation methods, particularly in the largely unexplored field of protein-protein interaction (PPI) representation learning for protein function prediction. Graph neural networks (GNNs), such as Graph Convolutional Networks (GCNs) [89], Graph Attention Networks (GATs),

and Graph Isomorphism Networks (GINs) [90], have shown promising results in predicting and utilizing PPIs for biomedical tasks. Applying these advanced graph-based representation learning methods to low-data protein function prediction is an area that has not been extensively explored yet. However, it has the potential to lead to significant improvements in performance and could be an exciting area of research.

In addition, current biomedical text-based representation methods are not ideal for handling long texts. For instance, the Longformer [57] and Reformer [57, 58] models are designed to handle long sequences of text effectively by combining global and local context. These models offer an opportunity to enhance the performance of large language models trained on biomedical data by incorporating global context awareness.

Overall, this study highlights the need for continued research in multimodal representation learning methods, particularly in the field of protein function prediction, and suggests potential avenues for further improvement and exploration in the field. The use of advanced models, such as GNNs, VAEs, GANs and other generative model types offers exciting possibilities for improving performance and generating high-quality representations. This study encourages researchers to explore these areas and further develop modern fusion strategies for explicitly modeling complex cross-modal interactions. The development of multi-task multimodal learning frameworks could also help the model better understand multimodal contents and lead to further improvements in performance.

5 Methods

5.1 A Summary of the Benchmark Dataset and Evaluation Metrics

Gene Ontology (GO) a standardized system for the functional annotation of genes and their products. It is a comprehensive, hierarchical vocabulary of terms that describe the molecular functions (MF), biological processes (BP), and cellular components (CC) associated with genes and gene products across different organisms [6]. In our recent study, we developed the PROBE (Protein RepresentatiOn BEnchmark) tool consisting of a dataset and evaluation method used to assess the performance of alternative protein representation methods including prediction of GO term annotations [45]. In the PROBE, the ontology-based PFP benchmark dataset was created by using human proteins and their GO term annotations. The data was preprocessed based on predetermined filtering rules to improve the reliability of the annotations. The GO terms were then grouped according to the number of annotated proteins and the depth of the term in the GO graph, and a selection of dissimilar terms was chosen from each group. The final dataset consists of 125 GO terms (Supplementary Table S8, S9), each with a list of annotated proteins, and is used to evaluate the performance of various methods for predicting GO terms. Specifically, we obtained human proteins and their corresponding GO term annotations from

reliable databases, excluded electronically made annotations to ensure data quality, created individual lists for each GO term, filtered proteins using UniRef clusters to eliminate bias, and grouped GO terms based on their number of annotated proteins and specificity (Supplementary Table S10). By applying a meticulous approach, we established 27 distinct GO term groups and selected five dissimilar terms from each group to construct a total of 500 prediction models. Additionally, we incorporated three rule/association-based methods and evaluated performance through 5-fold cross-validation. Detailed information on the dataset and the evaluation methods can be found in the next subsections.

In our study, we utilized weighted F1 scores as well as accuracy, hamming distance, precision and recall to assess the performance of protein representations in the context of protein function prediction. The weighted F1 score is a measure of the effectiveness of a classifier that takes into account the relative importance of each label, as well as the number of true positive, false positive, and false negative predictions made by the classifier. This measure is particularly useful in a multi-label setting such as GO term prediction, where multiple GO terms may be assigned to a single protein, and the relative importance of each term may vary. To calculate the weighted F1 score, we first determined the F1 score for each GO term. The weighted F1 score is then calculated as the mean of all per-class F1 scores, with the weights for each term determined based on the support of the class.

5.2 Calculation of Sequence-based Representations

In our study, we generated protein sequence-based representations by adopting the results of our recent PROBE (Protein RepresentatiOn BEnchmark) study [45]. To obtain the protein sequences for our analysis, we used the UniProt database [91], which is a widely used resource for gathering standardized protein sequences. We used canonical protein sequences which allowed us to ensure the consistency of our calculations across all proteins.

To generate the sequence representations, we employed 24 representation learning methods, including both classical (e.g., alignment-based, physicochemical) and artificial learning-based approaches (Supplementary Table S1a). Artificial learning-based methods (15 of 24) took the protein sequences as input and utilized techniques such as deep learning and natural language processing to extract relevant features of the proteins. These features were then mapped onto a continuous vector space using techniques like word embeddings or neural network architectures. The resulting feature vectors captured various inherent properties of the proteins, including structural and functional information.

It is worth noting that some of the representation learning methods we used in this study were specifically designed to generate protein-level representations, while others were intended to generate residue-level representations. For residue-level representations, we utilized the mean pooling technique to combine the information from all the residues in the protein and obtain overall protein representations. Additionally, we carefully considered the source data and algorithmic approaches used by the various representation learning methods in

order to cover a wide range of methodologies and ensure the comprehensiveness of our results. Details can be found in the methods section of the PROBE study. Detailed information about sequence representations that we utilized in our study can be found in the Methods section.

5.3 Calculation of Protein-Protein Interaction-based Representations

Graphs are a powerful way to represent information that has connections, and PPI data is a good example of this. In PPI data, proteins are represented as nodes and their interactions as edges. Machine learning algorithms can then be applied to these graph representations to make predictions about protein interactions. One common way to do this is by transforming the graph into a low-dimensional vector representation, which allows the algorithm to generalize the input data and make predictions. These representations, called graph embeddings, can be created using various techniques such as Node2Vec [48], HOPE [47] in which we used this study.

Node2Vec learns vector representations in a similar way to how word2vec [49] learns the vector representations of words (i.e. both use the skip-gram model [49]).

The Node2Vec method consists of three steps:

Sampling: A graph is sampled using random walks.

Training skip-gram: The random walks used in the sampling process can be thought of as a sentence made up of words, where each node represents a word and each walk results in a sequence of nodes. These node sequences are used for the training of the skip-gram model.

Calculation of representation vectors: Protein representations are the outputs of the hidden layer in the skip-gram model. When a relevant node is given as input, the output is a vector that represents that node. In this study, each node represents a protein and each edge represents an interaction between these proteins.

Node2Vec models each node as a protein, and each sequence of nodes visited during a walk is modeled as a sequence. Node2Vec creates node sequences using the Breadth First Search (BFS) and Depth First Search (DFS) [48] search algorithms. The innovative part of Node2Vec is its sampling strategy, which it performs using a random walk strategy on the graph. Graph traversal is the act of moving intentionally along the nodes and edges of a graph for a specific purpose, while preserving the neighborhoods and structures. To do this, an appropriate path is needed to explore the graph. BFS and DFS use second-order random walks to discover neighbors, discover distant neighborhoods and sample the graph. BFS starts from the starting node and expands outward to all nodes at the same distance before moving on to the next. DFS starts from the starting node and explores as far as possible along each branch before backtracking.

Node2Vec uses a biased random walk strategy (tuned via hyperparameters) that allows the search to focus on the structure of the graph. Node2Vec has two hyperparameters, p and q , that control the sampling strategy. p controls the return probability (i.e. probability of returning to the previous node) and q controls the probability of moving to a neighbor node. If $p < q$, the search is more likely to continue moving outward from the current node, and if $p > q$, it is more likely to search around the local area. When $p = q$, the search is unbiased and has an equal chance of moving outward or returning. In other terms these parameters determine exploration of local and global context.

In the second step Node2Vec uses the skip-gram model to generate representation vectors. The model has a well known general NN structure. Firstly, the model is fed forward with the input data. The loss is calculated, and then the weights are updated based on this loss. This process is repeated for a certain number of epochs. In this process, $w(t)$ is the input, or target word. There is a hidden layer where a projection takes place between the input vector $w(t)$ and the weight matrix. The output of this operation in the hidden layer is then transferred to the output layer. The output layer performs the calculation between the output vector of the hidden layer and the weight matrix of the output layer. Then, in the given context, the softmax activation function is applied to calculate the probability of the words within the relevant window for the input $w(t)$. As a result, when any node is taken as input, a vector of size equal to the number of unique nodes containing the probability values of the nodes is obtained. Additionally, \mathbf{V} is the known as the node distribution of the system in the node sequence, and N is the number of neurons in the hidden layer. The size of an input vector is $|\mathbf{V}|$, and each node is encoded using one-hot encoding. The weight matrix for the hidden layer (\mathbf{W}) is of size $|\mathbf{V}| \times N$. The product of \mathbf{W} and the hidden layer gives a output vector of size $|\mathbf{V}|$.

The HOPE (Higher-Order Proximity Embedding) method is a graph representation technique that aims to preserve the second-order proximity between nodes, which is the relationship between the neighbors of a node. The HOPE method preserves this proximity by considering the sum of the singular values of the submatrices formed by the rows and columns of the adjacency matrix corresponding to the neighbors of a node. To obtain the vector representations, the HOPE method reduces the resulting matrix to a d -dimensional vector using singular value decomposition (SVD). This allows the method to capture the inherent structure of the graph in a low-dimensional space, making it suitable for various downstream tasks such as node classification and link prediction.

One advantage of the HOPE method is that it can be applied to both undirected and directed graphs, making it a versatile tool for representing a wide range of complex data structures. Additionally, the method is computationally efficient, making it suitable for large-scale graph representation learning tasks. Existing methods are unable to preserve the critical feature of directed graphs, known as asymmetric transitivity. Asymmetric transitivity refers to the correlation between directed edges, meaning that if there is a directed path from u to v , then there is likely to be a directed edge from u to v . To overcome this challenge, the preservation of asymmetric transitivity is based on the use of High-Order Proximity preserved Embedding (HOPE). The hyperparameter β in HOPE is a

distortion parameter. It determines how quickly the weight of a path decreases as the path length increases.

In the present study, the HOPE algorithm was implemented in Python using the NetworkX [92] library. The resulting vector representations were used as input for prediction models in the study. Overall, the HoPE method provided robust and informative vector representations that captured the inherent structure of the protein-protein interaction graphs.

The Node2Vec algorithm was applied to protein-protein interaction graphs obtained from the IntACT database². The original size of the file was 1063382 rows and 42 columns. The ID(s) interactor A and ID(s) interactor B columns were filtered, reducing the data to two dimensions (1,063,382 rows by 2 columns).

If the both interactions were not represented by uniprot ids, these lines were filtered. Also, duplicates were then removed, and the remainder was 587,777 interactions. Moreover, we only select human proteins which left 16,435 nodes (proteins) and 241,833 interactions.

We used our benchmarking tool PROBE to assess alternative hyper parameter combinations of HOPE and Node2Vec. The hyper parameters used are shown in Supplementary Table S5 and Supplementary Table S6 in the supplementary material. We calculated alternative representations for the same protein dataset utilizing each hyper parameter tuned model. Afterwards, we calculated F1 scores for each alternative representation. All combinations of dimension (d) and β were tested for HOPE and all combinations of d , p and q were tested for Node2Vec. We present results of the best 10 representations of HOPE and Node2Vec in Figure 3 and Supplementary Table S1b.

5.4 Calculation of Text Representations

Protein-related information is widely available in the literature in the form of text. However, the systematic processing of this data remains an open problem. In our study, we aimed to process this data using the UniProtKB/Swiss-Prot database and PubMed as data sources. The UniProtKB/Swiss-Prot database is particularly useful because the information it contains has been summarized by experts from the literature and entered into the UniProtKB/Swiss-Prot database.

As part of our study, we downloaded all protein records (entries) for all species in xml format from the UniProtKB/Swiss-Prot database as of June 2020. These species include archaea, bacteria, fungi, humans, invertebrates, mammals, plants, rodents, vertebrates, viruses, and unclassified species. A total of 562,253 records were downloaded. For each of these records, we created text files with the file headers being the UniProt IDs.

We then extracted the “Function”, “Cofactor”, “Subunit”, “Tissue Specificity”, “Induction”, “Domain”, “PTM”, and “Disease” sub-sections of the “Comments”

²The `intact.zip` file was downloaded on 07.07.2020 from the IntAct Molecular Interaction Database. Preprocessing was performed on the `intact.txt` file within the zip file.

section (i.e., `<comment>`) of the downloaded records using the BioPython library. These subsections were saved in text format one after the other in separate files for each record. Of the downloaded records, 20,365 were identified as belonging to humans and we use these records to generate the text based protein representation vectors. We then used the UniProt IDs of these human protein records to prepare the text information for creating protein representations from the previously created folder containing the text information for all records. We also access PubMed papers referenced in these fields and download their abstracts. These abstracts were saved under a single file belonging to proteins. We created two datasets, (i) text gathered from UniProt, (ii) text gathered from UniProt and PubMed. Hence the vectors calculated using these two datasets were named as UNIPROT-VectorModelName and UNIPROT-PubMed-VectorModelName.

We used the BioBERT [54], BioWordVec [51], and BioSentVec [52] models to process the text information and create protein representation vectors. BioBERT is a pre-trained language model based on the BERT model, which was trained on a large biomedical corpus and fine-tuned on various biomedical tasks. BioWordVec and BioSentVec are word and sentence embedding models, respectively, that were trained on a large biomedical corpus. We used the BioBERT model to obtain contextualized word embeddings for each word in the text. The BioWordVec model was used to obtain word embeddings, and the BioSentVec model was used to obtain sentence embeddings. These embeddings were then summarised to form the final protein representation vectors. For this summarisation we used mean pooling over word vectors.

BioWordVec is a biomedical word embedding method that combines subword information from unlabeled biomedical text with a widely-used biomedical controlled vocabulary called Medical Subject Headings (MeSH). It is based on the fastText model and was trained on PubMed and MIMIC-III Clinical Database text corpora. The dimensions of the resulting word embeddings are 200, and the model was trained with a window size of 20, a learning rate of 0.05, a sampling threshold of 10^{-4} , and negative examples set to 10. BioWordVec has been shown to improve performance over the previous state of the art on a range of biomedical natural language processing (BioNLP) tasks.

BioSentVec is a biomedical sentence embedding method that is based on the sent2vec model. It was trained on the PubMed and MIMIC-III Clinical Database text corpora and produces 700-dimensional sentence embeddings. The model uses the bi-gram model and was trained with a window size of 20 and negative examples set to 10. BioSentVec has been shown to outperform other unsupervised and supervised methods on clinical sentence pair similarity tasks using the BIOSSES and MedSTS datasets. It has also been used to improve performance on a range of BioNLP tasks.

The BioWordVec and BioSentVec model was trained on the PubMed and MIMIC-III Clinical Database text corpora, with a total of 28,714,373 documents, 181,634,210 sentences, and 4,354,171,148 tokens in the PubMed corpus, and 2,083,180 documents, 41,674,775 sentences, and 539,006,967 tokens in the MIMIC-III Clinical notes corpus

Both BioWordVec and BioSentVec are useful for a variety of tasks in biomedical natural language processing, including document classification, information retrieval, and text summarization.

We used term frequency-inverse document frequency (TF-IDF) with principal component analysis (PCA) to generate representation vectors with dimensions of 256, 512, 768, and 1024. TF-IDF is a statistical measure that reflects the importance of a word in a document within a corpus, taking into account the frequency of the word in the document and the inverse frequency of the word across the entire corpus. By weighting the words in this way, TF-IDF can be used to identify the most important words in a document and filter out less important words. PCA is a statistical technique that is used to reduce the dimensionality of data by identifying the underlying patterns in the data and projecting the data onto a lower-dimensional space. In our study, we used PCA to reduce the dimensionality of the representation vectors generated from the TF-IDF matrix. By reducing the dimensionality of the vectors, we were able to capture the most important features of the data while eliminating less important features.

5.5 Calculation of Multimodal Representations

In this study, we develop three autoencoder-based methods for combining protein representations. Here, the input representation vectors are produced using text, aminoacid sequences, and protein-protein interactions which are denoted as \mathbf{i}_t , \mathbf{i}_s , \mathbf{i}_p respectively. Similarly, output representation vectors are denoted as \mathbf{o}_t , \mathbf{o}_s , \mathbf{o}_p .

The first method is a simple autoencoder (SimpleAE) that takes the concatenated form of the individual representation vectors as input. The middle layer of the trained autoencoder is intended to be used as a vector representing the protein, and is denoted as \mathbf{z}_{mid} . The input (\mathbf{v}_i) and output (\mathbf{v}_o) vectors in this model were concatenated as $\mathbf{v}_i = (\mathbf{i}_t, \mathbf{i}_s, \mathbf{i}_p)$ and $\mathbf{v}_o = (\mathbf{o}_t, \mathbf{o}_s, \mathbf{o}_p)$.

The second method is a multimodal autoencoder (MultiModalAE) that involves the reconstruction of individual representation vectors for the sequence, text, and protein-protein interaction data separately. In this case, again, \mathbf{z}_{mid} is also used as a vector representing the protein. Here the difference is each modality that each input is propagated independently up to the \mathbf{z}_{mid} layer. After the \mathbf{z}_{mid} layer, the modalities are again separated (see Figure 5b).

\mathbf{z}_{mid} was calculated by integrating each modality in a fully connected manner;

$$\mathbf{z}_{mid} = f_{text} \odot f_{sequence} \odot f_{PPI} \quad (1)$$

The third method, called sequence-based autoencoder (TransferAE), is created using transfer learning, in which the weights of a trained MultiModalAE model are transferred to another autoencoder model that takes protein sequence representation as input and generates representations for the text and protein-

protein interaction data. This method allows for the generation of protein representations for proteins for which data is only available in the form of sequence information.

The TransferAE model is created using transfer learning from the MultiModalAE model. Since the TransferAE model takes only sequence data as input, it starts as a subnetwork of the MultiModalAE model, excluding input layers for PPI, and text. Then the TransferAE is then further trained with sequence input only, so that it can learn to reconstruct the representation vectors for text and PPIs using only this input. The input sequence is also output by the network, for verification and error backpropagation. Like the MultiModalAE model, the TransferAE model also has multiple hidden layers with varying dimensions. For this model we transfer weights and biases of sequence input.

However for the decoder the output vectors are still \mathbf{o}_t , \mathbf{o}_s , \mathbf{o}_p . Here, we should note that decoder weights and biases for these modalities were transferred from MultiModalAE to TransferAE.

Alternative \mathbf{z}_{mid} dimensions (256, 512, 768, 1024) were tested for all models, in order to determine the optimal size for the representation vectors. The models are trained using the text sequence, PPI, and protein sequence representation vectors, and the performance of the models is evaluated using a weighted F1 score.

For all AE models we used the ReduceLROnPlateau function from the lr_scheduler module of PyTorch [93]. This function allows us to reduce the learning rate of the optimizer when the performance of the model plateaus, or stops improving. This can help prevent overfitting, and allows the model to continue learning and improving even when it is no longer making progress with the current learning rate.

The optimizer used in these models is the AdamW optimizer, which is a variant of the popular Adam optimizer that includes weight decay, which can help prevent overfitting by regularizing the model’s weights. The learning rate for the AdamW optimizer is set to 1e-3, which is a common choice for many deep learning models.

The loss function used in these models is the mean squared error (MSE) loss [94], which is a common choice for regression tasks. MSE loss is calculated by taking the squared difference between the predicted and true values, and averaging the squared differences over all examples in the dataset. This loss function is sensitive to large errors, and can be effective at encouraging the model to make small, precise predictions.

Overall, the combination of the ReduceLROnPlateau function, AdamW optimizer, and MSE loss function can be effective at training deep learning models for regression tasks, such as protein representation generation. These components can help the model learn effectively, prevent overfitting, and make accurate predictions.

5.6 The Methodology for the Immune-escape Protein Prediction

This case study aimed to predict new immune escape proteins in lung adenocarcinomas, a cancer type with a high mortality rate, using a prediction model with a low amount of training data. The study utilized TCGA-LUAD RNA-Seq data to calculate differentially expressed genes, resulting in 1434 genes, of which 329 were low, and 1105 were highly expressed in lung adenocarcinoma tumors compared to the matched normal lung tissue (Supplementary File 1). A negative dataset was created using GO BP ontology-based similarities between proteins and semantic similarity calculations to known immune-escape proteins. Multimodal protein representation vectors with autoencoders were generated using protein sequence, PPI, and text data. Finally, the study utilized autoencoder-based representation to train immune-escape predictors models using fully connected feed-forward neural networks (FC-NN) to predict new immune-escape proteins. The study predicted 121 immune-escape proteins (Supplementary Table S3) from the differentially expressed gene set, and the predictions were evaluated via literature search and existing functional annotations in source databases.

The aim of the first phase was to identify differentially expressed genes between tumor and normal tissue samples for the purpose of selecting immune-escape protein candidates. To achieve this goal, the TCGA-LUAD (The Cancer Genome Atlas Lung Adenocarcinoma) data was downloaded from the TCGA database [95] using the TCGABiolinks package [96]. The RNA-Seq method, with Illumina HiSeq as the sequencing platform, was chosen as the experimental method for the data set. TCGABiolinks allows for searching, downloading, and analyzing data from the National Cancer Institute database using the GDC Application Programming Interface (API) with R programming [97].

Here we first filtered data based on read count and then modeled data using the General Linear Model (GLM). The "quantile" method was used in the filtering phase. To use this method, a cut-off value for the read count in RNA-Seq analysis must be determined. In this study, this value was set to 0.25 (`qnt.cut=0.25`). Thus, the 25th percentile of the data frame representing each row as a gene was determined. The "glmLRT" method was used in the differential gene expression analysis phase [98]. This model fits the read counts to a negative binomial distribution [99] and performs ANOVA-style tests [100]. The "glmLRT" method used in this study, using the GLM, checks for differences between groups to determine whether there is a difference in expression between tumor and normal tissue. After the data distribution model is created with GLM in this phase, the hypothesis test is performed with the log-odds ratio. The p-value and adjusted p-value (false discovery rate – FDR) for each gene are calculated in this test.

The immune-escape protein candidates were selected using gene expression analysis with the aim of identifying tumor immune-escape proteins among the proteins encoded by differentially expressed genes. The TCGA-LUAD data was downloaded from the TCGA database using the TCGABiolinks package and the RNA-Seq method with the Illumina HiSeq platform was chosen as the

experimental method for the data set. The "quantile" and "glmLRT" methods were used in the implementation of gene expression analysis in R. The "quantile" method was used in the filtering phase, and the "glmLRT" method was used in the differential gene expression analysis phase. The genes over 2 fold-change and FDR is smaller than 0.01 were considered as differentially expressed. This set was used as input for the immune-escape prediction model later.

The positive samples in the training set were gathered by an exhaustive literature search. Which are; IL10, IL2, CD44, TGFB1, IL12A, SELL, PTGES2, IFNG, EBAG9, VEGFA, CXCR1, CXCR2, LMP1, CTLA4, ARG1, PSMB8, IDO1, HLA-G, TAP1, ICAM1, FASLG, IKBKB, CD80, CD274, CD44, CAMP, TNFRSF6B, FOXP3, CD47 [101, 102, 103, 104, 105, 106, 107, 108, 109])

A set of negative examples was created for the training of a classifier. This set was obtained from To this end, a semantic similarity matrix based on the Gene Ontology (GO) was first constructed. The Lin similarity [65] from the GoSemSim package [110] was used to independently calculate the real GO-based semantic similarities between all proteins in the BP (biological process) category. Only protein-GO tags approved by human curators were used in these similarity calculations. The Lin similarity is based on Shannon's information theory, which states that the information content (IC) of an event is inversely proportional to the probability (P) of observing the event. Another concept used in the Lin similarity is the least common subsumer (LCS), which is the first common ancestor of two GO terms in the hierarchical GO graph when going to the root. The BP-based similarity matrix contains 6154 proteins. There are 26 immune-escape proteins (Supplementary Table S11) that can be represented by the vector of any of the three protein representation methods in the immune-escape list. First, the proteins for which the vector was calculated by all three protein representation methods were selected from the 6154 proteins. Subsequently, these proteins were filtered to ensure that they had a maximum of 50% sequence similarity with UniRef50 [111]. After this process, half of the remaining proteins with the highest average semantic distance from the immune-escape proteins were selected, and 124 proteins were randomly chosen from this group (Supplementary Table S12). In this way, a set of 124 proteins that are assumed not to participate in immune-escape processes was obtained. Overall, there are 26 positive and 124 negative samples used for training with available text, sequence and PPI data.

On the immune-escape prediction model training we first create a baseline model. We utilized SeqVec for protein sequence representation, BioBERT for text representation, and Node2Vec for protein-protein interaction (PPI) representation. We have selected our best autoencoder-based representation (i.e., MultiModalAE-256) for low-data on the GO BP category. We utilized fully connected feed-forward neural networks (FC-NN). For the model we calculate, precision, recall, F1-Micro, F1-Macro, F1-Weighted and F-Max scores. We trained the model within a hyperparameter search using 5-Fold cross validation. During the hyperparameter search the goal was maximizing the F-Max score. At the end of the parameter search we refit each model with all data before predicting the immune-escape protein candidates. The detailed results can be found in the Supplementary Table S7.

References

- [1] I Friedberg. *Automated protein function prediction—the genomic challenge*. 2006.
- [2] Amarda Shehu, Daniel Barbará, and Kevin Molloy. *A Survey of Computational Methods for Protein Function Prediction*. 2016.
- [3] Stavros Makrodimitris, Roeland C H J van Ham, and Marcel J T Reinders. “Automatic Gene Function Prediction in the 2020’s”. en. In: *Genes* 11.11 (Oct. 2020), p. 1264.
- [4] Naihui Zhou et al. “The CAFA challenge reports improved protein function prediction and new functional annotations for hundreds of genes through experimental screens”. en. In: *Genome Biol.* 20.1 (Nov. 2019), pp. 1–23.
- [5] Michael Ashburner et al. “Gene Ontology: tool for the unification of biology”. en. In: *Nat. Genet.* 25.1 (May 2000), pp. 25–29.
- [6] Gene Ontology Consortium. “The Gene Ontology resource: enriching a GOld mine”. en. In: *Nucleic Acids Res.* 49.D1 (Jan. 2021), pp. D325–D334.
- [7] Maria Littmann et al. “Embeddings from deep learning transfer GO annotations beyond homology”. en. In: *Sci. Rep.* 11.1 (Jan. 2021), pp. 1–14.
- [8] Shuwei Yao et al. “NetGO 2.0: improving large-scale protein function prediction with massive sequence, text, domain, family and network information”. en. In: *Nucleic Acids Res.* 49.W1 (May 2021), W469–W475.
- [9] Ronghui You et al. “DeepGraphGO: graph neural network for large-scale, multispecies protein function prediction”. en. In: *Bioinformatics* 37.Supplement_1 (July 2021), pp. i262–i271.
- [10] Bilwaj Gaonkar et al. “Deep learning in the small sample size setting: cascaded feed forward neural networks for medical image segmentation”. en. In: *Medical Imaging 2016: Computer-Aided Diagnosis*. Vol. 9785. SPIE, Mar. 2016, pp. 646–653.
- [11] Wartini Ng et al. “The influence of training sample size on the accuracy of deep learning models for the prediction of soil properties with near-infrared spectroscopy data”. en. In: *SOIL* 6.2 (Nov. 2020), pp. 565–578.
- [12] Ahmet Sureyya Rifaioglu et al. “DEEPred: Automated Protein Function Prediction with Multi-task Feed-forward Deep Neural Networks”. en. In: *Sci. Rep.* 9.1 (May 2019), pp. 1–16.
- [13] Maxat Kulmanov and Robert Hoehndorf. “DeepGOZero: improving protein function prediction from sequence and zero-shot learning based on ontology axioms”. en. In: *Bioinformatics* 38.Suppl 1 (June 2022), pp. i238–i245.
- [14] Hanwen Xu and Sheng Wang. “ProTranslator: Zero-Shot Protein Function Prediction Using Textual Description”. en. In: *Res. Comput. Mol. Biol.* (2022), pp. 279–294.
- [15] Megan Stanley et al. “FS-Mol: A Few-Shot Learning Dataset of Molecules”. In: *Thirty-fifth Conference on Neural Information Processing Systems Datasets and Benchmarks Track (Round 2)*. Nov. 2021.

- [16] Rahmad Akbar et al. “In silico proof of principle of machine learning-based antibody design at unconstrained scale”. en. In: *MABs* 14.1 (Jan. 2022), p. 2031482.
- [17] Milad Mostavi et al. “CancerSiamese: one-shot learning for predicting primary and metastatic tumor types unseen during model training”. en. In: *BMC Bioinformatics* 22.1 (May 2021), pp. 1–17.
- [18] Max Schwarzer et al. “Data-Efficient Reinforcement Learning with Self-Predictive Representations”. In: *arXiv preprint arXiv:2007.05929* (July 2020).
- [19] Joshua Meier et al. “Language models enable zero-shot prediction of the effects of mutations on protein function”. In: *Adv. Neural Inf. Process. Syst.* 34 (Dec. 2021).
- [20] Jiang Peiran et al. “FSL-Kla: A few-shot learning-based multi-feature hybrid system for lactylation site prediction”. In: *Comput. Struct. Biotechnol. J.* 19 (Jan. 2021), pp. 4497–4509.
- [21] Iman Deznabi et al. “DeepKinZero: zero-shot learning for predicting kinase-phosphosite associations involving understudied kinases”. en. In: *Bioinformatics* 36.12 (June 2020), pp. 3652–3661.
- [22] Emaad Khwaja, Yun S Song, and Bo Huang. “CELL-E: Biological Zero-Shot Text-to-Image Synthesis for Protein Localization Prediction”. en. In: *bioRxiv* (May 2022), p. 2022.05.27.493774.
- [23] Shaoxun Liu, Yi Kou, and Lin Chen. “Novel Few-Shot Learning Neural Network for Predicting Carbohydrate-Active Enzyme Affinity Toward Fructo-Oligosaccharides”. en. In: *J. Comput. Biol.* 28.12 (Dec. 2021), pp. 1208–1218.
- [24] Hitoshi Iuchi et al. “Representation learning applications in biological sequence analysis”. In: *Comput. Struct. Biotechnol. J.* 19 (Jan. 2021), pp. 3198–3208.
- [25] Jesse Vig et al. “BERTology Meets Biology: Interpreting Attention in Protein Language Models”. In: *International Conference on Learning Representations*. Feb. 2022.
- [26] Ashish Vaswani et al. “Attention Is All You Need”. In: (June 2017).
- [27] Tristan Bepler and Bonnie Berger. “Learning the protein language: Evolution, structure, and function”. In: *Cell Systems* 12.6 (June 2021), 654–669.e3.
- [28] Bruce J Wittmann, Yisong Yue, and Frances H Arnold. “Informed training set design enables efficient machine learning-assisted directed protein evolution”. In: *Cell Systems* 12.11 (Nov. 2021), 1026–1045.e7.
- [29] Wenzhong Guo, Jianwen Wang, and Shiping Wang. “Deep Multimodal Representation Learning: A Survey”. In: *IEEE Access* 7 (2019), pp. 63373–63394.
- [30] Tadas Baltrusaitis, Chaitanya Ahuja, and Louis-Philippe Morency. “Multimodal Machine Learning: A Survey and Taxonomy”. en. In: *IEEE Trans. Pattern Anal. Mach. Intell.* 41.2 (Feb. 2019), pp. 423–443.

- [31] Siddhant M Jayakumar et al. “Multiplicative interactions and where to find them”. In: (2020).
- [32] Weiyao Wang, Du Tran, and Matt Feiszli. “What Makes Training Multi-Modal Classification Networks Hard?” In: (May 2019). arXiv: 1905.12681 [cs.CV].
- [33] Yao-Hung Hubert Tsai et al. “Multimodal Transformer for Unaligned Multimodal Language Sequences”. In: *Proceedings of the 57th Annual Meeting of the Association for Computational Linguistics*. Florence, Italy: Association for Computational Linguistics, July 2019, pp. 6558–6569.
- [34] Zhen Xu, David R So, and Andrew M Dai. “MUFASA: Multimodal Fusion Architecture Search for Electronic Health Records”. In: (Feb. 2021). arXiv: 2102.02340 [cs.LG].
- [35] Dorothea Scheunemann et al. “Effect of Imbalanced Charge Transport on the Interplay of Surface and Bulk Recombination in Organic Solar Cells”. In: (May 2019). arXiv: 1905.01268 [physics.app-ph].
- [36] Itai Gat et al. “Removing bias in multi-modal classifiers: Regularization by maximizing functional entropies”. In: (Oct. 2020), pp. 3197–3208. arXiv: 2010.10802 [cs.CV].
- [37] Paul Pu Liang et al. “MultiBench: Multiscale Benchmarks for Multimodal Representation Learning”. In: (July 2021). arXiv: 2107.07502 [cs.LG].
- [38] Ying Li et al. “Capsule-LPI: a LncRNA-protein interaction predicting tool based on a capsule network”. en. In: *BMC Bioinformatics* 22.1 (May 2021), p. 246.
- [39] Pengwei Hu et al. “Learning Multimodal Networks From Heterogeneous Data for Prediction of lncRNA-miRNA Interactions”. en. In: *IEEE/ACM Trans. Comput. Biol. Bioinform.* 17.5 (Sept. 2020), pp. 1516–1524.
- [40] Fei He et al. “Large-scale prediction of protein ubiquitination sites using a multimodal deep architecture”. en. In: *BMC Syst. Biol.* 12.Suppl 6 (Nov. 2018), p. 109.
- [41] Da Zhang and Mansur Kabuka. “Multimodal deep representation learning for protein interaction identification and protein family classification”. en. In: *BMC Bioinformatics* 20.Suppl 16 (Dec. 2019), p. 531.
- [42] Yang Xue et al. “Multimodal Pre-Training Model for Sequence-based Prediction of Protein-Protein Interaction”. In: (Dec. 2021). arXiv: 2112.04814 [q-bio.BM].
- [43] Ying Li et al. “De novo Prediction of Moonlighting Proteins Using Multimodal Deep Ensemble Learning”. en. In: *Front. Genet.* 12 (Mar. 2021), p. 630379.
- [44] Shuangjia Zheng et al. “Deep scaffold hopping with multimodal transformer neural networks”. en. In: *J. Cheminform.* 13.1 (Nov. 2021), p. 87.
- [45] Serbulent Unsal et al. “Learning functional properties of proteins with language models”. en. In: *Nature Machine Intelligence* 4.3 (Mar. 2022), pp. 227–245.

- [46] Ahmed Elnaggar et al. *ProtTrans: Towards Cracking the Language of Lifes Code Through Self-Supervised Deep Learning and High Performance Computing*. en. <https://ieeexplore.ieee.org/document/9477085>. Accessed: 2022-9-12. July 2022.
- [47] Mingdong Ou et al. *Asymmetric Transitivity Preserving Graph Embedding*. en. <https://dl.acm.org/doi/10.1145/2939672.2939751>. Accessed: 2022-9-12. Aug. 2016.
- [48] Aditya Grover and Jure Leskovec. “node2vec: Scalable Feature Learning for Networks”. en. In: *KDD 2016* (Aug. 2016), pp. 855–864.
- [49] Chris McCormick. *Word2Vec tutorial -the skip-gram model*. https://www.fer.unizg.hr/_download/repository/TAR-2020-reading-05.pdf. Accessed: 2023-3-18. 2016.
- [50] Akiko Aizawa. *An information-theoretic perspective of tf-idf measures*. 2003.
- [51] Yijia Zhang et al. “BioWordVec, improving biomedical word embeddings with subword information and MeSH”. en. In: *Sci Data* 6.1 (May 2019), p. 52.
- [52] Qingyu Chen, Yifan Peng, and Zhiyong Lu. *BioSentVec: creating sentence embeddings for biomedical texts*. 2019.
- [53] Mahdi Naser Moghadasi and Yu Zhuang. *Sent2Vec: A New Sentence Embedding Representation With Sentimental Semantic*. 2020.
- [54] Jinhyuk Lee et al. “BioBERT: a pre-trained biomedical language representation model for biomedical text mining”. en. In: *Bioinformatics* 36.4 (Feb. 2020), pp. 1234–1240.
- [55] Jacob Devlin et al. “BERT: Pre-training of Deep Bidirectional Transformers for Language Understanding”. In: (Oct. 2018). arXiv: 1810.04805 [cs.CL].
- [56] Alex Wang et al. “GLUE: A Multi-Task Benchmark and Analysis Platform for Natural Language Understanding”. In: (Apr. 2018). arXiv: 1804.07461 [cs.CL].
- [57] Iz Beltagy, Matthew E Peters, and Arman Cohan. “Longformer: The Long-Document Transformer”. In: (Apr. 2020). arXiv: 2004.05150 [cs.CL].
- [58] Nikita Kitaev, Łukasz Kaiser, and Anselm Levskaya. “Reformer: The Efficient Transformer”. In: (Jan. 2020). arXiv: 2001.04451 [cs.LG].
- [59] Swagarika Jaharlal Giri et al. “MultiPredGO: Deep Multi-Modal Protein Function Prediction by Amalgamating Protein Structure, Sequence, and Interaction Information”. en. In: *IEEE J Biomed Health Inform* 25.5 (May 2021), pp. 1832–1838.
- [60] Vladimir Gligorijevic, Meet Barot, and Richard Bonneau. “deepNF: deep network fusion for protein function prediction”. en. In: *Bioinformatics* 34.22 (Nov. 2018), pp. 3873–3881.
- [61] Laurens van der Maaten and Geoffrey Hinton. “Visualizing Data using t-SNE”. In: *J. Mach. Learn. Res.* 9.86 (2008), pp. 2579–2605.

- [62] *Cancer mortality for common cancers*. en. <https://www.cancerresearchuk.org/health-professional/cancer-statistics/mortality/common-cancers-compared>. Accessed: 2023-3-18. May 2015.
- [63] Gregory L Beatty and Whitney L Gladney. “Immune Escape Mechanisms as a Guide for Cancer Immunotherapy”. en. In: *Clin. Cancer Res.* 21.4 (Feb. 2015), pp. 687–692.
- [64] The Cancer Genome Atlas Research Network. “Comprehensive genomic characterization of squamous cell lung cancers”. en. In: *Nature* 489.7417 (Sept. 2012), pp. 519–525.
- [65] Dekang Lin et al. “An information-theoretic definition of similarity”. In: *Icml*. Vol. 98. 1998, pp. 296–304.
- [66] Yoshihiro Ohue and Hiroyoshi Nishikawa. “Regulatory T (Treg) cells in cancer: Can Treg cells be a new therapeutic target?” en. In: *Cancer Sci.* 110.7 (July 2019), pp. 2080–2089.
- [67] Yudan Zeng et al. “Prognostic and Immunological Roles of MMP-9 in Pan-Cancer”. en. In: *Biomed Res. Int.* 2022 (Feb. 2022), p. 2592962.
- [68] Rafael Fridman et al. “Cell surface association of matrix metalloproteinase-9 (gelatinase B)”. en. In: *Cancer Metastasis Rev.* 22.2-3 (2003), pp. 153–166.
- [69] Ming O Li and Richard A Flavell. “TGF-beta: a master of all T cell trades”. en. In: *Cell* 134.3 (Aug. 2008), pp. 392–404.
- [70] Peter A van Dam et al. “RANK-RANKL Signaling in Cancer of the Uterine Cervix: A Review”. en. In: *Int. J. Mol. Sci.* 20.9 (May 2019).
- [71] Bhavjinder K Dhillon et al. “Systems Biology Approaches to Understanding the Human Immune System”. en. In: *Front. Immunol.* 11 (July 2020).
- [72] Kazi Mokim Ahmed et al. “Glutathione peroxidase 2 is a metabolic driver of the tumor immune microenvironment and immune checkpoint inhibitor response”. en. In: *J Immunother Cancer* 10.8 (Aug. 2022).
- [73] Qishun Geng et al. “COL1A1 is a prognostic biomarker and correlated with immune infiltrates in lung cancer”. en. In: *PeerJ* 9 (Mar. 2021), e11145.
- [74] Benjamin Wilde and Antonios Katsounas. “Immune Dysfunction and Albumin-Related Immunity in Liver Cirrhosis”. en. In: *Mediators Inflamm.* 2019 (Feb. 2019), p. 7537649.
- [75] Kiran Kurmi and Marcia C. Haigis. “Nitrogen Metabolism in Cancer and Immunity”. In: *Trends in Cell Biology* 30.5 (2020), pp. 408–424. ISSN: 0962-8924. DOI: <https://doi.org/10.1016/j.tcb.2020.02.005>. URL: <https://www.sciencedirect.com/science/article/pii/S0962892420300404>.
- [76] Dan He et al. “Pentose Phosphate Pathway Regulates Tolerogenic Apoptotic Cell Clearance and Immune Tolerance”. en. In: *Front. Immunol.* 12 (Jan. 2022).
- [77] Oleksiy Gryshchenko et al. “Calcium Signaling in Pancreatic Immune Cells”. en. In: *Function (Oxf)* 2.1 (2021), zqaa026.

- [78] Stefan Hirschmeier et al. “Improving Recall and Precision in Unsupervised Multi-Label Document Classification Tasks by Combining Word Embeddings with TF-IDF”. In: *ECIS 2020 Research Papers* (2020).
- [79] Haihua Chen et al. “A comparative study of automated legal text classification using random forests and deep learning”. In: *Inf. Process. Manag.* 59.2 (Mar. 2022), p. 102798.
- [80] Victor Sanh et al. “DistilBERT, a distilled version of BERT: smaller, faster, cheaper and lighter”. In: (Oct. 2019). arXiv: 1910.01108 [cs.CL].
- [81] Don Tuggener et al. “LEDGAR: A Large-Scale Multi-label Corpus for Text Classification of Legal Provisions in Contracts”. In: *Proceedings of the Twelfth Language Resources and Evaluation Conference*. 2020, pp. 1235–1241.
- [82] A Elnaggar et al. “ProtTrans: Toward Understanding the Language of Life Through Self-Supervised Learning”. In: *IEEE Trans. Pattern Anal. Mach. Intell.* 44.10 (Oct. 2022).
- [83] Sijie Mai et al. “Excavating multimodal correlation for representation learning”. In: *Inf. Fusion* 91 (Mar. 2023), pp. 542–555.
- [84] Qiang Cui et al. “MV-RNN: A Multi-View Recurrent Neural Network for Sequential Recommendation”. In: *IEEE Trans. Knowl. Data Eng.* 32.2 (Feb. 2020), pp. 317–331.
- [85] Kevin E Wu et al. “BABEL enables cross-modality translation between multiomic profiles at single-cell resolution”. In: *Proceedings of the National Academy of Sciences* 118.15 (2021), e2023070118.
- [86] Yangtao Wang et al. “Cross-modal fusion for multi-label image classification with attention mechanism”. In: *Comput. Electr. Eng.* 101 (July 2022), p. 108002.
- [87] Michalis Angelou et al. “Graph-based multimodal fusion with metric learning for multimodal classification”. In: *Pattern Recognit.* 95 (Nov. 2019), pp. 296–307.
- [88] Andreas Holzinger et al. “Towards multi-modal causability with Graph Neural Networks enabling information fusion for explainable AI”. In: *Inf. Fusion* 71 (July 2021), pp. 28–37.
- [89] Ming Chen et al. “Simple and Deep Graph Convolutional Networks”. In: *Proceedings of the 37th International Conference on Machine Learning*. Ed. by Hal Daumé Iii and Aarti Singh. Vol. 119. Proceedings of Machine Learning Research. PMLR, 2020, pp. 1725–1735.
- [90] Wen Zhong et al. “Long-distance dependency combined multi-hop graph neural networks for protein-protein interactions prediction”. en. In: *BMC Bioinformatics* 23.1 (Dec. 2022), p. 521.
- [91] UniProt Consortium. “UniProt: a worldwide hub of protein knowledge”. en. In: *Nucleic Acids Res.* 47.D1 (Jan. 2019), pp. D506–D515.
- [92] Aric Hagberg, Pieter Swart, and Daniel S Chult. *Exploring network structure, dynamics, and function using networkx*. en. Tech. rep. LA-UR-08-05495; LA-UR-08-5495. Los Alamos National Lab. (LANL), Los Alamos, NM (United States), Jan. 2008.

- [93] Sagar Imambi, Kolla Bhanu Prakash, and G R Kanagachidambaresan. “Py-Torch”. In: *Programming with TensorFlow: Solution for Edge Computing Applications*. Ed. by Kolla Bhanu Prakash and G R Kanagachidambaresan. Cham: Springer International Publishing, 2021, pp. 87–104.
- [94] David A Harville and Daniel R Jeske. “Mean Squared Error of Estimation or Prediction under a General Linear Model”. In: *J. Am. Stat. Assoc.* 87.419 (Sept. 1992), pp. 724–731.
- [95] Cancer Genome Atlas Research Network. “Comprehensive molecular profiling of lung adenocarcinoma”. en. In: *Nature* 511.7511 (July 2014), pp. 543–550.
- [96] Mohamed Mounir et al. “New functionalities in the TCGAblinks package for the study and integration of cancer data from GDC and GTEx”. en. In: *PLoS Comput. Biol.* 15.3 (Mar. 2019), e1006701.
- [97] Robert C Gentleman et al. “Bioconductor: open software development for computational biology and bioinformatics”. en. In: *Genome Biol.* 5.10 (Sept. 2004), R80.
- [98] Y Chen et al. “edgeR: Empirical analysis of digital gene expression data in R”. In: *Version: Release (3.12)* ().
- [99] Xu Ren and Pei-Fen Kuan. “Negative binomial additive model for RNA-Seq data analysis”. en. In: *BMC Bioinformatics* 21.1 (May 2020), p. 171.
- [100] Ellen R Girden. *ANOVA: Repeated Measures*. en. SAGE, 1992.
- [101] S. Brandau et al. “Myeloid-derived suppressor cells in the peripheral blood of cancer patients contain a subset of immature neutrophils with impaired migratory properties”. In: *Journal of Leukocyte Biology* 89.2 (2011), pp. 311–317. DOI: 10.1189/jlb.0310162.
- [102] Martin R. Jandus et al. “Lung Cancer: A Classic Example of Tumor Escape and Progression While Providing Opportunities for Immunological Intervention”. In: *Clinical and Developmental Immunology 2012* (2012), p. 160724. DOI: 10.1155/2012/160724.
- [103] D. Hunn and V. Bronte. “Immune suppressive mechanisms in the tumor microenvironment”. In: *Current Opinion in Immunology* 39 (2016), pp. 1–6. DOI: 10.1016/j.coi.2015.10.009.
- [104] Dass S. Vinay et al. “Immune evasion in cancer: Mechanistic basis and therapeutic strategies”. In: *Seminars in Cancer Biology* 35 (2015), S185–S198. DOI: 10.1016/j.semcancer.2015.03.004.
- [105] K. Leone, C. Poggiana, and R. Zamarchi. “The Interplay between Circulating Tumor Cells and the Immune System: From Immune Escape to Cancer Immunotherapy”. In: *Diagnostics* 8.3 (2018), p. 59. DOI: 10.3390/diagnostics8030059.
- [106] Renxiang Huang et al. “Loss of Fas expression and high expression of HLA-E promoting the immune escape of early colorectal cancer cells”. In: *Oncology Letters* 13 (2017), pp. 3379–3386. DOI: 10.3892/ol.2017.5921.
- [107] E. Carosella et al. “Systematic Review of Immunotherapy in Urologic Cancer: Evolving Roles for Targeting of CTLA-4, PD-1/PD-L1, and HLA-G”. In: *European Urology* 68.2 (2015), pp. 267–279. DOI: 10.1016/j.eururo.2015.02.040.

- [108] S. Zelenay et al. “Cyclooxygenase-Dependent Tumor Growth through Evasion of Immunity”. In: *Cell* 162 (2015), pp. 1257–1270. DOI: 10.1016/j.cell.2015.08.015.
- [109] E. A. Kotteas et al. “The Intercellular Cell Adhesion Molecule-1 (ICAM-1) in Lung Cancer: Implications for Disease Progression and Prognosis”. In: *Anticancer Research* 34.9 (2014), pp. 4665–4672.
- [110] Guangchuang Yu et al. “GOSemSim: an R package for measuring semantic similarity among GO terms and gene products”. en. In: *Bioinformatics* 26.7 (Apr. 2010), pp. 976–978.
- [111] B. E. Suzek et al. “UniRef clusters: a comprehensive and scalable alternative for improving sequence similarity searches”. In: *Bioinformatics* 31.6 (2015), pp. 926–932. DOI: 10.1093/bioinformatics/btu739.